LA-UR-17-23122 (Accepted Manuscript)

Room temperature thermal conductivity measurements of neat MOF-5 compacts with high pressure hydrogen and helium

Semelsberger, Troy Allen

To be published in: International Journal of Hydrogen Energy

DOI to publisher's version: 10.1016/j.ijhydene.2015.12.059

Permalink to record: http://permalink.lanl.gov/object/view?what=info:lanl-repo/lareport/LA-UR-17-23122

Room Temperature Thermal Conductivity Measurements of Neat MOF-5 Compacts with High Pressure Hydrogen and Helium

Troy A. Semelsberger[a,*], Mike Veenstra[b] and Craig Dixon[c]

[a] *Materials Physics and Applications Division, Los Alamos National Laboratory, P.O. Box 1663, Mail Stop K763, Los Alamos, NM 87545, USA*

[b] *Ford Motor Company, Research and Advanced Engineering, Dearborn, MI 48121, USA*

[c] *ThermTest Inc, 34 Melissa Street, Unit 1, Fredericton, NB E3A 6W1, Canada*

Abstract

Metal-organic frameworks (MOFs) are a highly porous crystalline material with potential in various applications including on-board vehicle hydrogen storage for fuel cell vehicles. The thermal conductivity of MOFs is an important parameter in the design and ultimate performance of an on-board hydrogen storage system. However, in-situ thermal conductivity measurements have not been previously reported. The present study reports room temperature thermal conductivity and thermal diffusivity measurements performed on neat MOF-5 cylindrical compacts (ρ = 0.4 g/mL) as a function of pressure (0.27–90 bar) and gas type (hydrogen and helium). The transient plane source technique was used to measure both the non-directional thermal properties (isotropic method) and the directional thermal properties (anisotropic method). High pressure measurements were made using our in-house built low-temperature, high pressure thermal conductivity sample cell. The intrinsic thermal properties of neat MOF-5 measured under vacuum were— Isotropic: $k_{isotropic}$ = 0.1319 W/m K, $\alpha_{isotropic}$ = 0.4165 mm^2/s; Anisotropic: k_{axial} = 0.1477 W/m K, k_{radial} = 0.1218 W/m K, α_{axial} = 0.5096 mm^2/s, and α_{radial} = 0.4232 mm^2/s. The apparent thermal properties of neat MOF-5 increased with increasing hydrogen and helium pressure, with the largest increase occurring in the narrow pressure range of 0–10 bar and then monotonically asymptoting with increasing pressures up to around 90 bar. On average, a greater than two-fold enhancement in the apparent thermal properties was observed with neat MOF-5 in the presence of helium and hydrogen compared to the intrinsic values of neat MOF-5 measured under vacuum. The apparent thermal properties of neat MOF-5 measured with hydrogen were higher than those measured with helium, which were directly related to the gas-specific thermal properties of helium and hydrogen. Neat MOF-5 exhibited a small degree of anisotropy under all conditions measured with thermal conductivities and diffusivities in the axial direction being higher than those in the radial direction. The low temperature specific heat capacities of neat MOF-5 were also measured and reported for the temperature range of 93–313 K (-180–40 °C).

Keywords: thermal conductivity, thermal diffusivity, MOF-5, high pressure, material properties, fuel cells, hydrogen, adsorbents, heat capacity, anisotropic, hydrogen storage

Corresponding Author, troy@lanl.gov, Phone: 505-665-4766

1.0 Introduction

A potential on-board hydrogen storage method for fuel cell vehicles is physical adsorption (alternatively called physisorption or cryo-adsorption) which stores hydrogen in the micropores of these porous materials. Metal-organic frameworks (MOFs) are leading candidates for physisorption-based hydrogen storage. The advantage of a sorption storage using MOFs is the hydrogen density within the micropores can significantly exceed that of the bulk gas at low pressures. In order to maximize the storage density, the hydrogen binding energy is enhanced through thermal management. In particular, the uptake of hydrogen by the MOF can be significantly reduced due to the increase in temperature which occurs during fueling from the heat of adsorption. In the same respect, the decrease in temperature due to the release of hydrogen reduces the usable capacity as result of the higher binding energy at low temperatures within the MOF. Typically, these sorption systems incorporate a heat exchanger within the material bed for managing the temperature during hydrogen fueling and delivery. The thermal conductivity properties have a direct influence on the system design and performance. When incorrectly determined, the heat exchanger could be over-designed which adds unnecessary weight, cost, and complexity or underperform which will increase the fueling times and reduce storage capacity along with the transient response of the material. Due to their high porosity, it is not uncommon for MOFs to have poor heat conduction properties. As a counter-measure, material enhancements (e.g. graphite) can be added to the material to form a composite to increase their thermal conductivity. These enhancement materials typically displace the storage material, which results in a decrease in the system storage capacity and an increase in the system weight. Therefore, it is important to accurately measure thermal conductivity of neat MOF-5 without these enhancements in the actual storage gas at anticipated operating pressures. Our objectives in this study were:

- Measure the isotropic and anisotropic thermal properties (conductivity and diffusivity) of neat MOF-5 as a function of pressure (0.27–91 bar) and gas type (hydrogen and helium)
- Measure the specific heat capacities of neat MOF-5 in the temperature range of -180–40 °C
- Develop a viable methodology for measuring the thermal properties of porous adsorbents at elevated pressures (≤ 100 bar) that can be extended to measurements performed at low temperatures (77 K)

2.0 Experimental Framework

2.1 MOF-5 Samples: The neat MOF-5 samples used in this study were cylindrical compacts (provided by Ford Motor Company) of neat MOF-5 powder that was synthesized and supplied by BASF. MOF-5 (or IRMOF-1) has a framework structure formed by metal Zn_4O nodes with organic 1,4-benzene dicarboxylic acid linkers The physical properties of the engineered compacts of neat MOF-5 are detailed in Table 1. Shown in Figure 1a is a rudimentary diagram of the cylindrical compact showing the puck dimensions and the orientation of the axial and radial transport directions relative to the puck geometry. Neat MOF-5 compacts were pressed by Ford Motor Company using a Sintech model 30/G load frame with a 30,000 lb capacity load cell. The applied force was parallel to the axial direction.

Table 1. Physical properties of neat MOF-5 samples used for thermal property measurements

Properties of Neat MOF-5 Compacts		
Puck Diameter	5.0	cm
Puck Height	1.312	cm
Puck Volume (1 puck)	25.75	mL
Puck Mass (1 puck)	10.3	g
Puck Density	0.4	g/mL
Pore Volume[a]	1.22	mL/g
Surface Area[a]	2466	m^2/g

[a] *interpolated values from neat MOF-5 compacts with densities of 0.3 and 0.5 g/mL from Liu and Siegel*

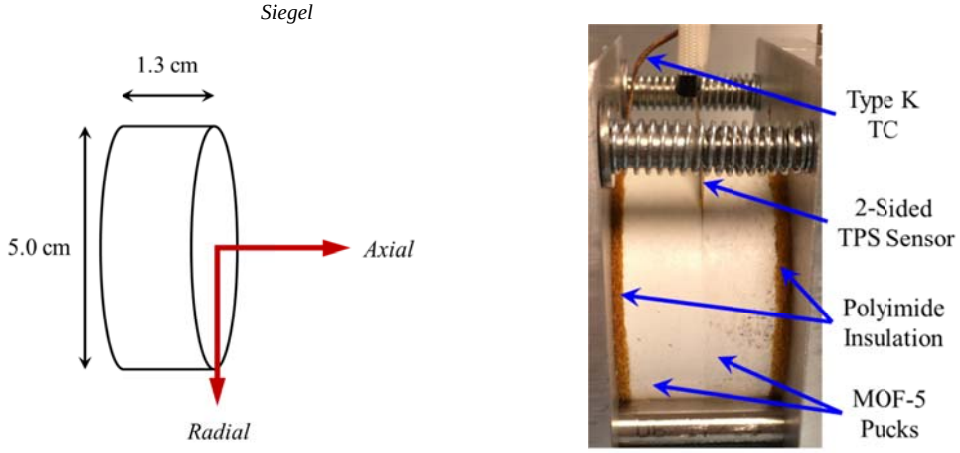

(a) (b)

Figure 1. (a) Rudimentary diagram illustrating the dimensions of the neat MOF-5 compacts (ρ = 0.4 g/mL) and the orientations of the axial and radial thermal transport properties relative to the puck geometry (b) sample arrangement detailing the two MOF-5 pucks, two-sided TPS sensor and the type K thermocouple used for standard isotropic and anisotropic thermal conductivity measurements

2.2 Specific Heat Capacity Measurements: Measurements of the specific heat capacities of neat MOF-5 were made on a Mettler-Toledo DSC 822 using the sapphire continuous Cp method. The heat capacities were measured in the temperature range of -180–40 °C with a ramp rate of 10°C/min. Sapphire (part #: ME-51140818) was used as the reference material for Cp determination of neat MOF-5. All samples and crucibles were thermally treated at 160 °C in a UHP nitrogen purged oven for two weeks prior to measurement. Measurements were performed in sealed 100 µL aluminum crucibles that were loaded and sealed in an argon purged glove box in order to maintain oxygen- and moisture-free samples. The mass of dried neat MOF-5 used was 38.77 mg. Two sapphire samples were used in the analysis, one as a reference and the other as a sample. The sapphire sample was used to validate the collected data by comparing the experimentally determined heat capacity of sapphire to the literature values [reference]. The dried mass of the sapphire reference was 23.77 mg and the dried mass of the sapphire sample was 47.22 mg. The readers are referred to the thesis "Heat Capacity Measurements of Porous Materials at Cryogenic Temperatures by Thea Ragna Storesund Mohn for a rigorous and thorough treatise on performing low temperature heat capacity measurements of porous adsorbent materials by differential scanning colorimetery [1].

2.3 Transient Plane Source (TPS) Thermal Property Measurements: Thermal conductivity measurements were performed at Los Alamos National Laboratory using a ThermTest TPS 2500S capable of measuring thermal conductivities from 0.001 to 1800 W/m K. A two-sided Kapton insulated TPS sensor, #5501 having a radius of 6.403 mm was used for the standard bulk isotropic and anisotropic measurements, TPS sensors are designed to be placed between the plane surfaces of two sample pieces of the material under investigation [2]. The basic assumption of the theory for the experimental technique is that the sensor is located in an infinite material. Two-sided sensor measurements offer high accuracy, repeatability, and flexibility in measurement temperature range. A two-sided sensor is preferred for measuring the anisotropic thermal properties. All measurements were taken with an arrangement where the two-sided senor was sandwiched between two identical neat MOF-5 pucks (refer to Figure 1b). The TPS technique is unique in its capability of measuring the thermal properties under elevated pressures and low temperatures.

The thermal property measurements were carried out using a LANL in-house built thermal conductivity sample cell capable of measuring thermal conductivities under elevated gas pressures (≤ 100 bar) at liquid nitrogen temperature. This study focused on measuring the thermal conductivities of neat MOF-5 as a function of hydrogen and helium pressure (0-100 bar) in the temperature range of 16-22°C. The sample temperature was monitored by a type K thermocouple that was directly affixed to the back side of the MOF-5 compact located between the sample and the polyimide insulation. The MOF-5 samples were clamped in the sample holder using four bolts tightened to a torque of 5 N·m. In an attempt to maintain a constant applied force on the sample over the temperature and pressure range investigated, we added 1/8" polyimide insulation (McMaster-Carr part #: 93015K62) to act as expansion joints (Figure 1b). The polyimide insulation also served as a gas diffusion layer. Thermally treated polyimide insulation (160°C for two weeks in a UHP N_2 purged oven) is shown as the brownish-orange material located between the stainless steel sample holder and the neat MOF-5 sample pucks. Because we measured the thermal conductivities of neat MOF-5 in the presence of hydrogen and helium under elevated pressures, the measured values should be viewed as "apparent" thermal conductivities of MOF-5 plus a gas-phase contribution. The pressure was monitored with a head mounted pressure gauge with a dial range of 0–150 bar. UHP Hydrogen and UHP helium with purities of 99.999% were used as the headspace gases. To ensure accuracy, thermal conductivity measurements were made under equilibrium, gradient-free conditions. For a given hydrogen or helium pressure, isothermal conditions were assured by waiting a minimum of 20 minutes between measurements. Measurements accompanying a change in headspace pressure were only made after a 40 minute equilibration period. The neat MOF-5 compacts were conditioned at 160 °C in a UHP N_2 purged oven for a minimum of two days followed by a 12 hour vacuum treatment (200 torr).

2.4 TPS Background: TPS Thermal transport property measurements were performed by locating the TPS sensor between identical MOF-5 samples to be measured. Previously mentioned, the solution of the thermal conductivity equation assumes the sensor is in an infinite medium. Knowing this is not the case, the measurement and subsequent analysis must account for the finite boundaries of the sample which is accomplished by ensuring the thermal penetration depth is less than the sample dimensions and the following criteria are met: the total to characteristic time [$F(\tau_a)$] is between 0.33–1.0, the overall temperature rise (ΔT) for the measurement is between 0.4–4 K, and the mean deviation of data scatter is 10^{-4} or better for the TPS 2500S system. The anisotropic thermal transport properties are determined from the standard analysis of bulk isotropic thermal properties (Equation 1–Equation 3).

Equation 1

$$\Delta T = \frac{P}{\pi^{3/2} \cdot r \cdot k_{isotropic}} \cdot F(\tau_a)$$

Equation 2

$$\tau_a = \sqrt{\frac{t}{\Theta_a}}$$

Equation 3

$$\Theta_a = \frac{r^2}{\alpha_a}$$

Where ΔT is the time dependent temperature increase of the sensor, P is the total power output of the sensor, r is the overall radius of the sensor heating source, k_a is the thermal conductivity in the axial direction, k_r is the thermal conductivity in the radial direction, $F(\tau_a)$ is the dimensionless time dependent function with respect to the axial direction in the sample, t is the measured time from the start of the transient recording, Θ_a is the characteristic time and α_a is the thermal diffusivity of the sample in the axial direction. Given the equations for the standard analysis of the bulk isotropic thermal properties and the user input of the volumetric heat capacity (ρC_p) of the sample, the anisotropic thermal transport properties can be calculated using Equation 4–Equation 7. *Note: the isotropic and anisotropic measurements performed in this study were separate and independent measurements.*

Anisotropic Equations

Equation 4

$$k_{isotropic} = A = \sqrt{k_a k_r}$$

Equation 5

$$\alpha_a = B = \frac{k_a}{\rho C_p}$$

Equation 6

$$k_r = \frac{A^2}{k_a} = \frac{A^2}{\rho C_p \cdot B}$$

Equation 7

$$\alpha_r = \frac{k_r}{\rho C_p} = \frac{A^2}{\left(\rho C_p\right)^2 \cdot B}$$

Evident from Equation 4–Equation 7, the volumetric heat capacity (ρC_p) is required to determine the axial and radial contributions of the thermal transport properties. The radial conductivity (Equation 6) and diffusivity (Equation 7) are inversely proportional to the volumetric heat capacity. As will be shown the volumetric heat capacity of our samples must not only take into account the neat MOF-5 compact, but also the contributions of helium and hydrogen contained within the void volume of the neat MOF-5 compact.

3.0 Results and Discussion

The transient plane source technique was used to measure the bulk isotropic and anisotropic thermal properties of our neat MOF-5 samples. The isotropic method does not require any *a priori* sample data in order to measure the bulk isotropic thermal conductivity. The anisotropic method, however, does require the input of the sample's volumetric heat capacity (denoted as ρC_p [=] MJ/m^3 K) at the pressure and temperature of interest prior to performing the anisotropic measurements. The volumetric heat capacity is the specific heat capacity (denoted as C_p [=] MJ/g K) multiplied by the density

of the sample (denoted as ρ [=] g/m^3). The volumetric heat capacity used in the calculations of the anisotropic properties must take into account the contributions of gas type (i.e., hydrogen or helium), gas pressure, and temperature. This is important because the volumetric heat capacity of the sample changes as a function of these variables. The sample is defined as the neat MOF-5 engineered compact plus the gas occupied within the neat MOF-5 compact. The sample density is also as a function of pressure and temperature which must also be taken into account in the volumetric heat capacity. Equation 8 is the general equation used to calculate the sample's volumetric heat capacity.

Equation 8

$$\left(\rho C_p\right)_{sample} = \bar{\rho}_{sample} \cdot \sum x_i C_{p,i}$$

$$i = hydrogen,\ helium,\ MOF-5$$

3.1 Sample Volumetric Heat Capacity (MJ/m^3 K): The pressure-dependent volumetric heat capacities used for the calculation of the anisotropic thermal properties are shown in Figure 2. The changes in sample's volumetric heat capacity as a function of pressure are appreciable compared to the volumetric heat capacity of neat MOF-5 (0.288 MJ/m^3 K) when the contributions of hydrogen and helium are taken into account. The gas phase contributions of hydrogen at 290 K and helium at 300 K resulted in approximately a 20% increase (a factor of 1.2) in the volumetric heat capacity at 100 bar for hydrogen and approximately 14% (a factor of 1.14) for helium. Further changes in the sample's volumetric heat capacity are expected as the temperature is decreased to more realistic adsorbent operating temperatures (~77 K). For example the sample's volumetric heat capacity increases by a factor of 22 with hydrogen at 100 bar and 77K; and by a factor of 11 for helium at 100 bar and 77 K. Consequently, ignoring the contributions of the gas phase component and gas type will result in erroneous data—this is especially true with adsorbents that have inherently low thermal properties (i.e., thermal conductivity and heat capacities). The largest contributor to changes in the sample's volumetric heat capacity can be attributed to the heat capacity of helium (5.19 J/g K at 300 K) and hydrogen (14.32 J/g K at 1 bar). Details on the approximations of the volumetric heat capacity as function of gas type, pressure, and temperature are shown below.

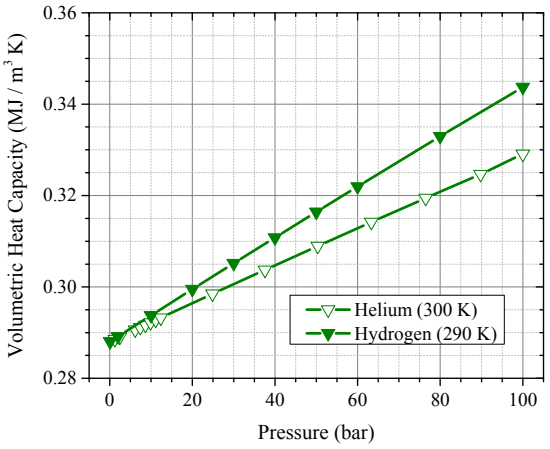

Figure 2. Calculated volumetric heat capacities of H_2/MOF-5 and He/MOF-5 samples as a function hydrogen pressure at 290 K and helium at 300 K. Volumetric heat capacities are used in the calculations of anisotropic thermal properties

The volumetric heat capacity of the sample was taken as the mass faction weighted mixture of hydrogen (or helium) and neat MOF-5 compact. Equation 8 can be rewritten as

Equation 9

$$\left(\rho C_p\right)_{sample} = \left[\frac{m_j(T,P) + m_{MOF}}{V_{total}}\right]\left[x_j C_{p,j}(T,P) + \left(1 - x_j\right) C_{p,MOF}(T)\right]$$

$$j = hydrogen\ or\ helium$$

3.2 Hydrogen and Helium Density: The first term on the right hand side (RHS) of Equation 9 is the sample density and was determined by the total mass (MOF-5 plus hydrogen or helium) divided by the total volume of the neat MOF-5 compacts (V_{total}). We used a two-sided measurement that incorporated two MOF-5 pucks with a fixed total mass and volume of 20.6 g and 51.4 mL, respectively. The volume of neat MOF-5 (V_{total} = 51.4 mL) was assumed constant and independent of applied gas pressure. The mass of hydrogen or helium (m_j) within the pores of neat MOF-5 was calculated using a pore volume of 1.22 milliliters per gram of MOF-5 which was determined by interpolating experimentally quantified pore volumes of neat MOF-5 at densities of 0.3 and 0.5 g / mL [3]. The pore volume was assumed to be the primary volume occupied by hydrogen or helium within the MOF-5 compacts. The total pore volume (V_{pore}) of neat MOF-5 with a density of 0.4 g / mL was calculated to be 25 mL. Given the high hydrogen or helium pressures of the experiments, we calculated the gas densities using the compressibility factor (Z-based) and the ideal gas law (IGL) to determine the most accurate calculation of gas densities and hence the mass of hydrogen or helium within the MOF-5 compacts. Compressibility factors for helium and hydrogen are from [4,5]. Although the calculated gas densities using the ideal gas law and the compressibility factor equations are not significantly different, we did however settle on using the gas densities calculated from the compressibility factors. Figure 3a and Figure 3b show the calculated pressure-dependent gas densities of helium and normal gaseous hydrogen used in this study

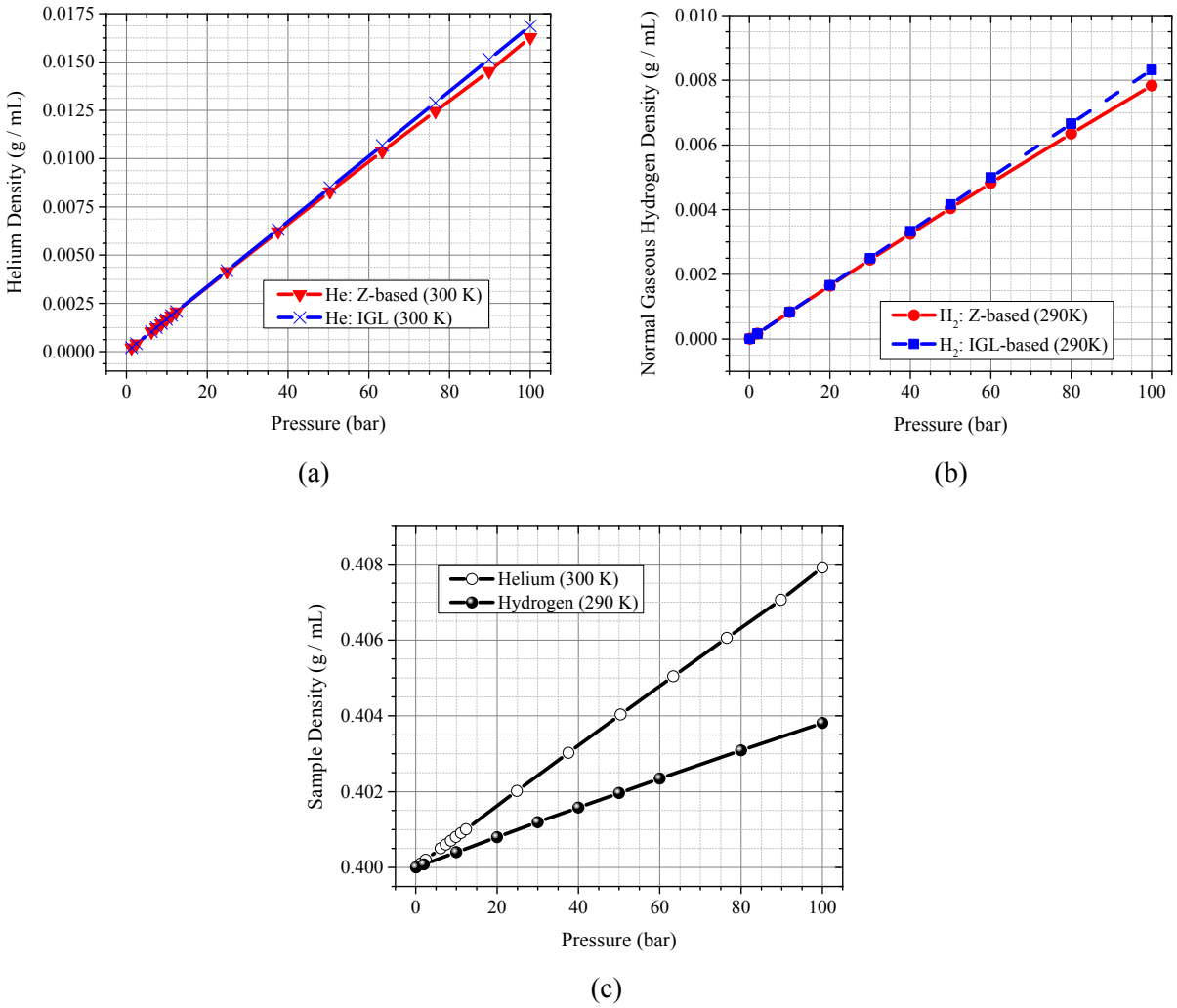

Figure 3. Gas density calculations using the ideal gas law (blue) and compressibility factors (red) as a function of pressure for (a) helium at 300 K and (b) hydrogen at 290 K; (c) Calculated sample densities of H_2/MOF-5 and He/MOF-5 samples as a function of hydrogen pressure at 290 K and helium pressure at 300 K (*note: sample density takes into account the mass of neat MOF-5 and the mass of hydrogen or helium contained within the pore volume of neat MOF-5)*

The mass of hydrogen or helium within neat MOF-5 compacts is simply the gas density (Figure 3a and Figure 3b) multiplied by the pore volume of neat MOF-5 (V_{pore} = 25 mL). Alternatively, the mass of any gas contained in a solid porous matrix with a known pore volume and compressibility factor can be calculated as a function of pressure and temperature using Equation 10.

Equation 10

$$m_j(T,P) = \frac{MW_j \cdot P}{Z_j RT} \cdot V_{pore}$$

$$j = adsorbate\ (H_2, He, \ldots)$$

Given the gas phase density of hydrogen and helium (Figure 3a and Figure 3b) and the total pore volume of neat MOF-5 compacts, the mass of hydrogen or helium contained within the compacts were calculated. The sample density (MOF-5 plus H_2 or He) was calculated by taking the sum of the masses of helium or hydrogen at the temperature and pressure of interest and adding it to the total mass of neat MOF-5 (20.6 g MOF-5) and dividing by the total volume of neat MOF-5 (51.4 mL). Shown in Figure 3c are the sample

densities (MOF-5 plus H_2 or He) as a function of pressure at a temperature of 290 K and 300 K, respectively. Given the masses of hydrogen or helium and neat MOF-5, the mass fractions were calculated and used to determine the mass fraction weighted heat capacities. The mass fractions of helium at 300 K ranged from 0% under vacuum to 1.9% at 100 bar; for hydrogen at 290 K the mass fractions ranged from 0% under vacuum to 0.9% at 100 bar. For adsorbent operating conditions of 77 K and 100 bar the mass fractions of helium and hydrogen are 5.5% and 3.5% , respectively. The mass fraction of gas contained within the neat MOF-5 puck volume was calculated using Equation 11. The mass fraction weighted heat capacity of the sample (second term on the RHS of Equation 9) requires known values of capacities for hydrogen, helium and neat MOF-5 at the pressure and temperature of interest.

Equation 11

$$x_j = \frac{m_j(T,P)}{m_{total}(T,P)} = \frac{\left(\frac{MW_j \cdot P}{ZRT}\right) \cdot V_{pore}}{\left(\frac{MW_j \cdot P}{ZRT}\right) \cdot V_{pore} + m_{MOF}}$$

$$j = hydrogen\ or\ helium$$

3.3 Neat MOF-5 Specific Heat Capacity (J/g K): The heat capacity of neat MOF-5 was assumed to be independent of applied gas pressure. The heat capacity of neat MOF-5 was measured at LANL as a function of temperature (-180–60 °C). Shown in Figure 4 are the results of the low temperature DSC measurements of neat MOF-5 and sapphire. For comparison, the literature values of sapphire [6] are also shown in Figure 4. The curve fit for the specific heat capacity of neat MOF-5 for the temperature range of -180–60 °C is shown in Table 2.

Table 2. Equation for the specific heat capacity of neat MOF-5

$C_p\big\vert_{MOF\text{-}5}(T) = B_0 + B_1T + B_2T^2 + B_3T^3 + B_4T^4 + B_5T^5 + B_6T^6$	
Coefficient	**Value**
B_0	0.69269
B_1	0.00189
B_2	-1.53E-05
B_3	1.49E-07
B_4	1.83E-09
B_5	4.83E-12
B_6	2.66E-15
Temperature range = -180 to 40 °C *Units: C_p [=] J/g K, T [=] °C* *Adjusted R^2 = 0.9998*	

The heat capacity of neat MOF-5 used in calculating the sample's volumetric heat capacity was 0.72 J/g K (T = 16 °C). Note: If additives (e.g, expanded natural graphite) are used to enhance MOFs, then the contributions of the additives should be taken into account as necessary when calculating the volumetric heat capacity.

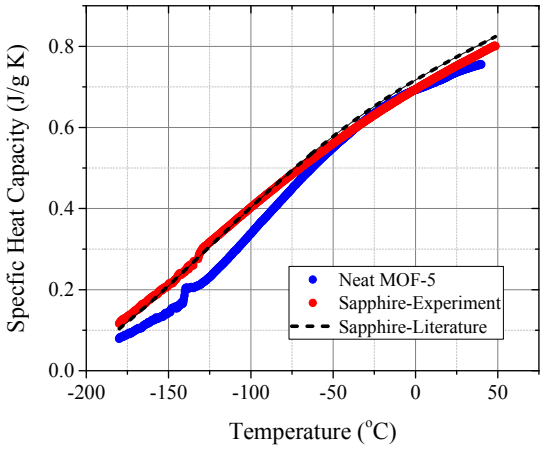

Figure 4. Experimentally determined specific heat capacities of neat MOF-5 (blue) and sapphire (red) [note: for reference the literature values of sapphire (black dashed line) are also shown [6]**]**

3.4 Hydrogen & Helium Heat Capacity (J/g K): The temperature and pressure dependent heat capacities of hydrogen and helium used were from the internally consistent data set from WADD Tech Report 66. According to WADD Tech report 66, the heat capacity of helium can be taken as independent of pressure and temperature. Deviations in helium heat capacity as a function of pressure from ambient to 100 bar deviate about 0.5% at room temperature and about 0.05% at 1000K [4]—for this reason we assumed a constant helium heat capacity of 5.19 J/g K over the entire pressure range investigated. The hydrogen heat capacity is a stronger function of temperature and pressure than that for helium. Heat capacity data for normal gaseous hydrogen pulled from WADD Tech Report is reproduced in Figure 5. Figure 5a, depicts the heat capacity of normal gaseous hydrogen as a function of pressure (0–100 atm) for the isotherms of 70–100 K and Figure 5b depicts the heat capacity as function of pressure (0–100 atm) for isotherms of 120–300 K. At 300K, the heat capacity of normal gaseous hydrogen does not deviate significantly within 0–100 bar hydrogen pressure. However, for temperatures below 100 K the heat capacities of hydrogen deviate significantly. For example, the heat capacity of normal gaseous hydrogen is 15.6 J/g K at 100 atm and 70 K; and 10.6 J/g K at 1 atm and 70 K. Figure 5c depicts the heat capacity of normal gaseous hydrogen as function of temperature for the isobars of 0-100 atm. The surface plot depicting the heat capacity of normal gaseous hydrogen as a function of temperature and pressure is shown in Figure 5d. The largest change in hydrogen heat capacity occurs with decreasing temperature at low hydrogen pressures (< 10 bar). Significant pressure dependent changes are observed in the hydrogen heat capacity for typical adsorbent operating temperatures in the range of 60–120 K. The surface fit for normal gaseous hydrogen is shown in Table 3. *Note: The hydrogen heat capacity surface fit in Table 3 must not be used for temperatures below 60 K.*

Table 3. Equation for the specific heat capacity of hydrogen as a function of temperature and pressure

$$C_p\big|_{H_2}(T,P) = a + b/T + cP + d/T^2 + eP^2 + fP/T + g/T^3 + hP^3 + iP^2/T + jP/T^2$$

Coefficient	Value
a	16.31225
b	-537.86149
c	-0.0068022856
d	-15170.24
e	8.8318439E-05
f	1.2640953
g	1744626.5
h	2.5356798E-08
i	-0.020856876
j	299.46402

Temperature range = 60–300 K
Pressure range = 1–100 atm
Units: C_p [=] J/g K, T [=] K, P[=] atm
Adjusted R^2 = 0.9955
Note: data fitted from [5]

Data for the specific heat capacities of hydrogen and helium were taken from [5]. The density of the sample was taken as the total mass of gas plus the mass of neat MOF-5 sample

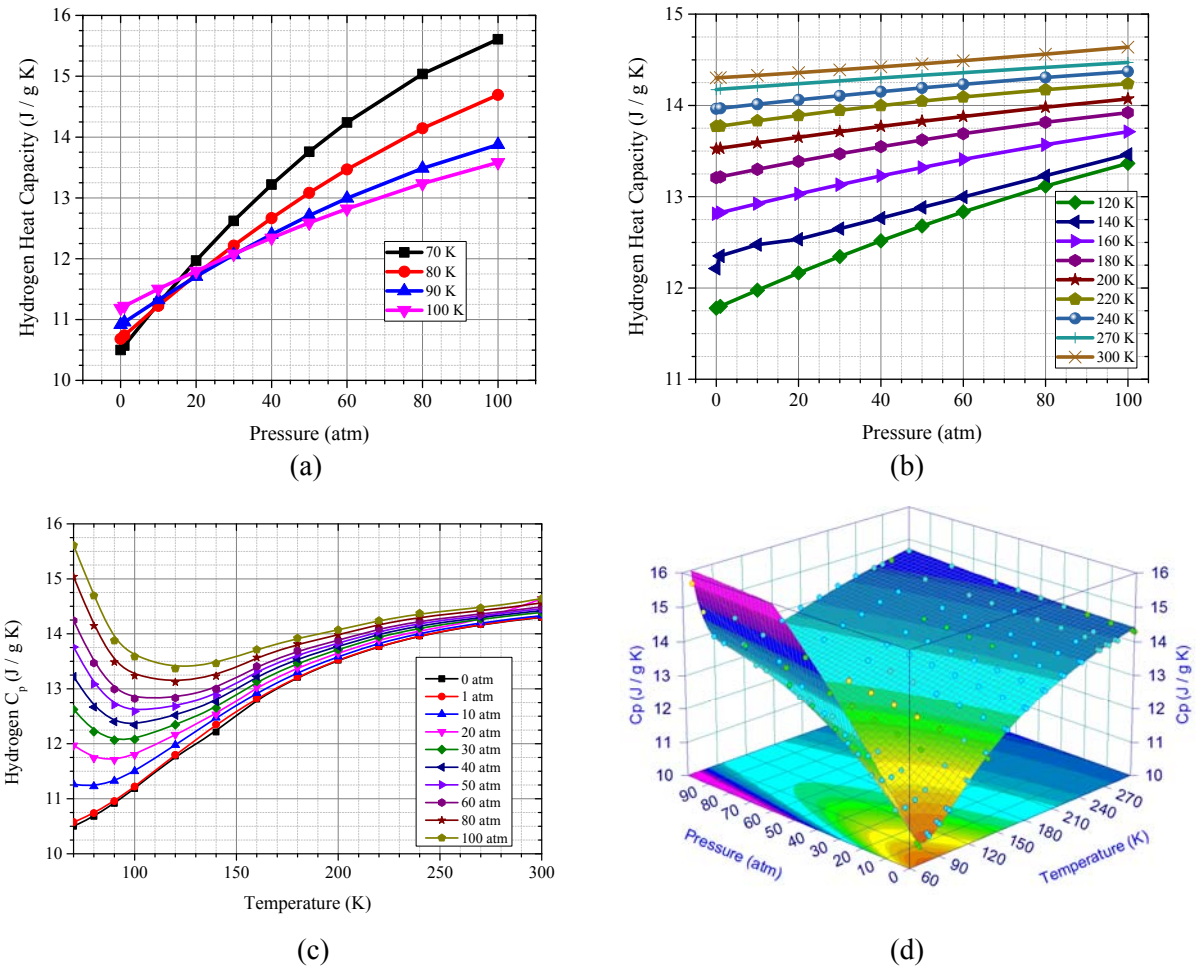

Figure 5. Specific heat capacities of normal gaseous hydrogen as a function of absolute pressure (1– 100 atm) and temperature: (a) for isotherms = 70–100 K, (b) for isotherms = 120–300 K; (c) plot of normal gaseous hydrogen heat capacity as function of temperature (70–300 K) for isobars = 1–100 atm; (d) surface plot of normal gaseous hydrogen heat capacity as function of temperature and pressure *(note: data reproduced from* [5]*)*

3.5 Bulk Isotropic Thermal Conductivity Data: Shown in Figure 6 are the bulk isotropic thermal conductivity results obtained as a function of pressure for both helium and hydrogen at 16 °C. In general, the observed thermal conductivities are well behaved and appear reasonable because the thermal conductivities demonstrate a sharp increase in thermal conductivity within a small window of increasing pressure from vacuum and then leveling off with further increases in pressure. In addition, the measured thermal conductivities also show the thermal conductivity effects of gas type. The average isotropic thermal conductivity of neat MOF-5 under vacuum at 16 °C was measured to be 0.1319 W/m K (12 data point average with a standard deviation of ± 0.0027 W/m K)—comparable to insulating brick at 0.15 W/m K at 25 °C. For both helium and hydrogen a sharp increase in thermal conductivity is observed with an increase in gas pressure from 0.27 bar ("vacuum") to around 20 bar. Increases in the gas pressure from 20 bar to 90 bar, resulted in relatively constant or limiting values in thermal conductivity. The limiting values of thermal conductivity for a pressure of 91 bar (abs) at 16 °C for hydrogen was 0.3336 W/m K and for helium the limiting value was around 0.2971 W/m K—comparable to Portland cement at 0.29 W/m K at 25 °C. The limiting values observed with hydrogen and helium can be attributed to the differing thermal conductivities of normal gaseous hydrogen and helium. The thermal conductivities of hydrogen (normal) and helium are reported to be 0.1767 W / m K [5] and 0.15 mW / m K [4] at 290 K (~16 °C) at or near 1 bar. There is close agreement when comparing the hydrogen to helium thermal conductivity ratios of the reported literature values to our thermal conductivity values measured at 3.72 bar (abs). The hydrogen to helium thermal conductivity ratio using the reported literature values at 1 bar and 290 K is 1.18 (= 0.1767 W/m K ÷ 0.15 W/m K). The thermal conductivity ratio of hydrogen to helium using our experimental data collected at 3.72 bar (abs) is 1.14 (= 0.2568 W/m K ÷ 0.2245 W/m K)—in close agreement with the ratio using the reported literature values. The average hydrogen to helium thermal conductivity ratio over the entire pressure range investigated at 16 °C was 1.10.

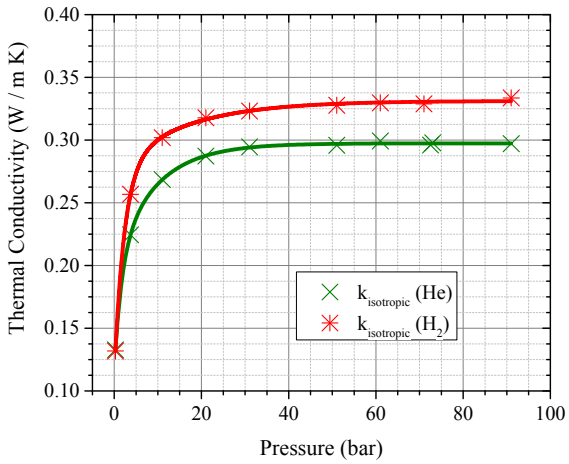

Figure 6. Isotropic (bulk) thermal conductivities of neat MOF-5 engineered compacts as a function of pressure (absolute) and gas type at 16 °C ***[all samples were treated in a UHP N2 purged oven at 160 °C for a minimum of two days, followed by vacuum treatment for 12 hrs; Average standard deviations for isotropic and anisotropic measurements were ±0.0052 W/m K (helium, 137 isotropic measurements) and ±0.0033 W/m K (hydrogen, 104 isotropic measurements]***

3.6 Bulk Isotropic Thermal Diffusivity Data: Figure 7 shows the bulk isotropic thermal diffusivities of neat MOF-5 as a function of helium and hydrogen pressure at 16 °C. Thermal diffusivity is the ratio of a materials ability to conduct heat relative to its ability to store heat and is calculated by dividing the thermal conductivity by the volumetric heat capacity. The salient feature of Figure 7 is the non-

monotonic nature of the thermal diffusivity curves. Figure 6 displays monotonically, asymptoting behavior while Figure 7 shows non-monotonic behavior. The isotropic thermal conductivities do not show definitive maxima within the pressure range investigated; however, there are definitive maxima in the thermal diffusivity curves. A maximum hydrogen thermal diffusivity 1.05 mm^2/s occurs around 20 bar and a maximum helium thermal diffusivity of 0.98 mm^2/s occurs around 30 bar. Increasing the gas pressure beyond the observed maxima, the thermal diffusivities continue to decrease up to the maximum pressure investigated. The monotonic, asymptoting behavior of the thermal conductivities in Figure 6 and the non-monotonic nature of the thermal diffusivities (Figure 7) could indicate that we are either underestimating the samples volumetric heat capacity for pressures below 30 bar and/or overestimating the sample's volumetric heat capacity for pressures greater than 30 bar. A 10% reduction in the volumetric heat capacity correlates to an 11% increase in the thermal diffusivity; while a 10% increase in volumetric heat capacity correlates to a 9% decrease in the thermal diffusivity.

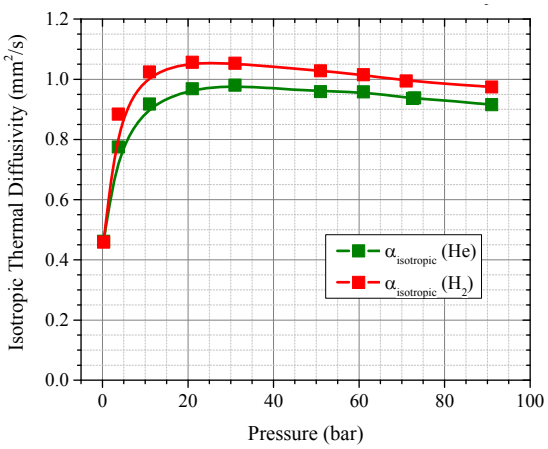

Figure 7. Isotropic (bulk) thermal diffusivities of neat MOF-5 engineered compacts as a function of pressure (absolute) at 16 °C for helium (green squares) and hydrogen (red squares) ***[Average standard deviations for isotropic thermal diffusivity measurements were ±0.0101 mm^2/s (helium, 137 isotropic measurements) and ±0.0134 mm^2/s (hydrogen, 104 isotropic measurements]***

3.7 Anisotropic Thermal Conductivity Data: Separate anisotropic measurements were performed to determine the radial and axial thermal conductivities of neat MOF-5 compacts under elevated hydrogen and helium pressures at 16 °C. The anisotropic measurements require the input of the sample's volumetric heat capacity (refer to Equation 4–Equation 7) in order to calculate the radial and axial contributions. The sample volumetric heat capacities used as inputs are shown Figure 2. Figure 8a shows the radial and axial thermal conductivities measured with neat MOF-5 as a function of helium pressure. Similar to the isotropic thermal conductivity curve with helium (Figure 6), the radial and axial thermal conductivity curves increase sharply from vacuum to around 10 bar and then are relatively constant with increasing pressure to 91 bar (abs). Anisotropic measurements performed under vacuum at 16 °C represent the axial and radial thermal conductivities of Neat MOF-5 in the absence of gas phase contributions (or at least limiting). The measured anisotropic thermal conductivities of neat MOF-5 under vacuum were 0.1477 W/m K (axial) and 0.1218 W/m K (radial). Although the samples are considered homogeneous, there are differing thermal conductivities observed in the radial and axial directions. The limiting values of the anisotropic thermal conductivities with helium at 16°C and 91 bar (abs) are 0.2723 W/m K (radial) and 0.3279 W/m K (axial). The origins of the differing radial and axial thermal conductivities are currently unverified. The numbers above the data points denote the order the anisotropic measurements were made—indicating the absence of hysteresis.

The anisotropic measurements of neat MOF-5 as a function of hydrogen pressure collected at 16 °C are shown in Figure 8b. Similar to the anisotropic thermal conductivity measurements with helium, the radial thermal conductivity is less than the axial thermal conductivity throughout the hydrogen pressure range investigated. In contrast to the anisotropic measurements with helium, the axial and radial thermal conductivities of neat MOF-5 diverge with increasing hydrogen pressures from 10–70 bar. For hydrogen pressures greater than 70 bar there may be some indication that the axial and radial thermal conductivities are leveling off or asymptoting. The limiting values for the axial and radial thermal conductivities of neat MOF-5 with hydrogen at 91 bar (abs) and 16 °C are 0.4504 W/m K (axial) and 0.2454 W/m K (radial). The divergent behavior observed with the axial and radial thermal conductivities of neat MOF-5 with hydrogen are unexpected and will be discussed below.

The dashed lines in Figure 8a and Figure 8b represent the average weighted contributions of the axial and radial thermal conductivities that would equal the measured isotropic values shown in Figure 6. The equation for the average weighted contributions of the axial and radial thermal conductivities is shown in Equation 12.

Equation 12

$$\left(k_{isotropic}\right)_i^{calc} = x_{avg} k_{axial,i} + \left(1 - x_{avg}\right) k_{radial,i}$$

The subscript i denotes the thermal conductivities collected as a function of pressure [i.e., 0.27, 2.72, 10, ... 90 bar (abs)]. The weighted contributions were calculated at each pressure (Equation 13) and then averaged over the total number of data point (denoted as n) to yield the average weighted contributions (Equation 14) of the axial and radial thermal conductivities.

Equation 13

$$\left(k_{isotropic}\right)_i^{exp} = \left(\left(xk_{axial}\right)_i + \left[\left(1 - x\right)\left(k_{radial}\right)\right]_i\right)_{anisotropic}^{exp}$$

Equation 14

$$x_{avg} = \frac{\sum x_i}{n}$$

The average weighted contributions of the axial and radial thermal conductivities agree well with the measured isotropic values (Figure 8c) for both hydrogen and helium. This analysis was performed as a check to see if the weighted contributions of the anisotropic thermal are independent of gas type. If the values don't match then this may suggest the sample integrity has been compromised (e.g., cracks, sensor displacement etc.). Interestingly, even though the axial and radial thermal conductivities diverge with hydrogen, the weighted contributions of the axial thermal conductivity (42%) and radial thermal conductivity (58%) agree well with the weighted percentages of the axial (43%) and radial thermal (57%) conductivities with helium—suggesting the sample integrity has not been compromised. The weighted contributions also indicate that the axial thermal conductivity is the dominant direction of thermal transport.

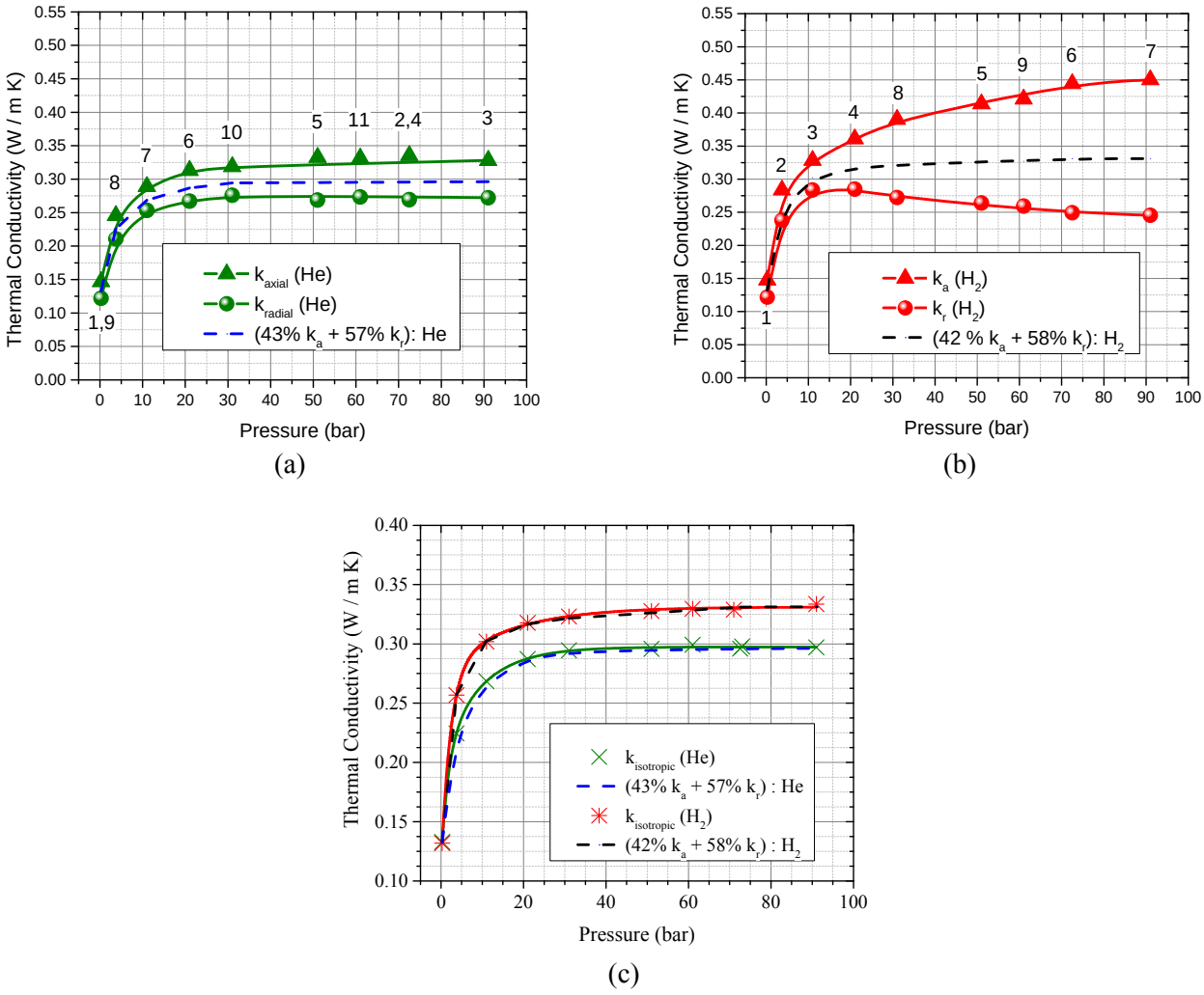

Figure 8. Anisotropic thermal conductivities of neat MOF-5 engineered compacts as a function of pressure (absolute) at 16 °C with (a) helium; (b) hydrogen; (c) Comparison of isotropic thermal conductivities to the average weighted contributions of the axial and radial anisotropic conductivities ***[note: all samples were treated in a UHP N_2 purged oven at 160 °C for a minimum of two days, followed by vacuum treatment for 12 hrs; Average standard deviations for isotropic and anisotropic measurements were ±0.0052 W/m K (helium, 137 measurements) and ±0.0033 W/m K (hydrogen, 104 measurements)]***

3.8 Anisotropic Thermal Diffusivity Data: The anisotropic thermal diffusivities of neat MOF-5 as a function of pressure for helium and hydrogen are shown Figure 9. Mentioned previously, the calculated sample volumetric heat capacities shown in Figure 2 were used for quantifying the anisotropic thermal diffusivities of neat MOF-5 with helium (Figure 9a) and hydrogen (Figure 9b). The observed trends in thermal diffusivity for both helium and hydrogen are similar to those observed for anisotropic thermal conductivities (Figure 8a and Figure 8b). The axial and radial thermal diffusivities of neat MOF-5 under vacuum were observed to be 0.5096 mm^2/s (axial) and 0.4232 mm^2/s (radial). The anisotropic thermal diffusivities of neat MOF-5 with helium demonstrated a maximum axial diffusivity around 1.0757 mm^2/s over the pressure range of 20–90 bar at 16 °C. The radial diffusivity of neat MOF-5 with helium had a maximum diffusivity of 0.9171 mm^2/s at 31 bar (abs) and 16 °C. The radial diffusivity of neat MOF-5 with helium continued to decrease with increasing helium pressure up to the maximum pressure investigated (91bar, abs) to a radial diffusivity value of 0.8375 mm^2/s.

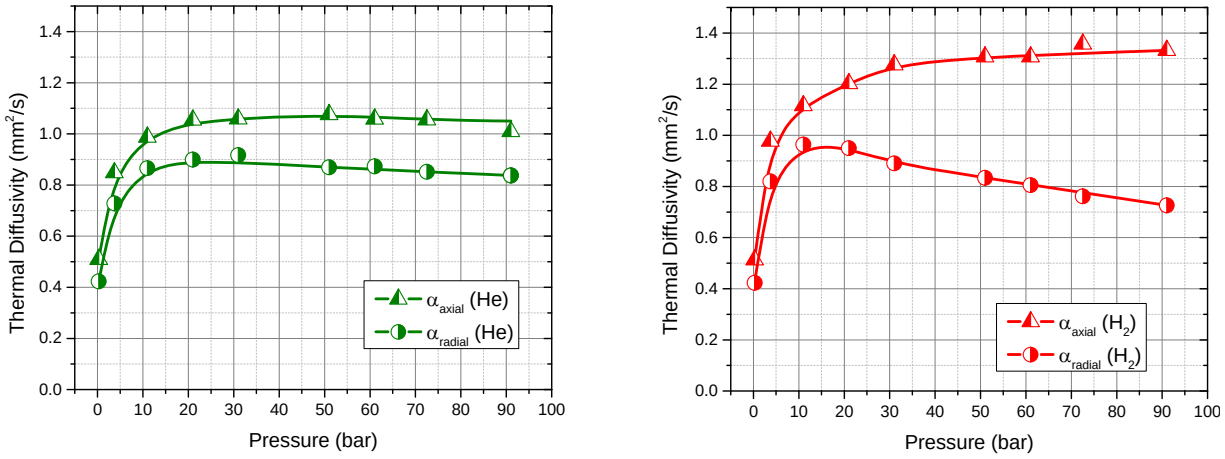

Figure 9. Anisotropic thermal diffusivities of neat MOF-5 engineered compacts as a function of pressure (absolute) at 16 °C for (a) helium and (b) hydrogen

The anisotropic thermal diffusivities of neat MOF-5 with hydrogen are shown in Figure 9b. The thermal diffusivities, similar to the anisotropic conductivities, diverge with increasing hydrogen pressures above 20 bar. A limiting value in the axial thermal diffusivity of neat MOF-5 with hydrogen of 1.3323 mm^2/s was observed at the maximum pressure investigated (91 bar absolute). The radial diffusivity curve of neat MOF-5 as a function of hydrogen pressure is non-monotonic exhibiting a maximum radial diffusivity of 0.9640 mm^2/s at 11 bar (abs). With increasing hydrogen pressure above 11 bar (abs) the radial diffusivities continue to decrease to a diffusivity value of 0.7262 mm^2/s at a hydrogen pressure of 91 bar (abs). In comparing the anisotropic thermal diffusivities collected with hydrogen and helium, the axial thermal diffusivity with hydrogen is around 24% higher than the axial diffusivity collected with helium. In contrast, the radial diffusivity with hydrogen is approximately 21% lower than the radial diffusivity collected with helium. The effects of gas type are expected because of the gas specific thermal properties of heat capacity, thermal conductivity and thermal diffusivity for hydrogen and helium

The isotropic (Figure 6 and Figure 7) and anisotropic (Figure 8a and Figure 9a) thermal properties of neat MOF-5 as a function of helium pressure at 16°C are, in general, well-behaved and expected; that is, monotonically increasing and asymptoting. The same can be said for the observed isotropic thermal properties of neat MOF-5 as a function of hydrogen pressure at 16 °C (Figure 6 and Figure 7). However, the anisotropic thermal properties measurements with neat MOF-5 as a function of hydrogen pressure at 16 °C (Figure 8b and Figure 9b) are in clear departure to what was observed with helium. There are no rational explanations for the anisotropic thermal properties of neat MOF-5 with

hydrogen to be non-monotonic. It is worth mentioning that to our knowledge this is the only research paper to report on thermal property measurements of neat MOF-5 (or any porous material) as a function of elevated hydrogen or helium pressure. For validation, TPS measurements were performed at ThermTest at ambient pressure and temperature (25 C) conditions with neat MOF-5 at the same density without the gas contribution. The results were consistent with the thermal conductivity of 0.14 W/m K for the axial and 0.12 W/m K for the radial direction. The sample tested was compacted with the same MOF-5 material and method although the dimensions were different using a sample with 1.3 cm diameter and 0.47 cm thickness. The anisotropic thermal diffusivities measured by ThermTest at ambient pressure were 0.4 mm^2/s for the axial and 0.36 mm^2/s for the radial direction. Beyond ambient pressures, there are no data to compare to in order to determine what should or should not be expected. Therefore, we report an internally consistent thermal property data set for both helium and hydrogen, using an identical approach to data treatment and property estimation for both helium and hydrogen; which is documented in this manuscript. This does not preclude us from presenting some thoughts on possible explanations on the unexpected anisotropic results observed with neat MOF-5 as a function of hydrogen pressure as compared to the other data.

Two scenarios exist with respect to the anisotropic data with hydrogen—the data are either accurate or inaccurate. If the anisotropic data for neat MOF-5 with hydrogen are accurate, then there exists underlying phenomena causing the divergent behavior in the anisotropic thermal properties of neat MOF-5 with hydrogen which needs to be identified. Possible causes could include molecular interactions of hydrogen with MOF-5 and/or preferential crystal orientation upon compaction. The preferential orientation upon MOF-5 compaction seems unlikely because this phenomenon would be invariant to the gas type and thus observed with helium. The fact that the discrepancy in anisotropic data is only observed with hydrogen indicates that hydrogen specific molecular interactions with MOF-5 cannot be discounted as a possible contributor.

If the anisotropic data for neat MOF-5 with hydrogen are inaccurate, then this could be the result of inaccurate property estimation of the sample's volumetric heat capacity and/or the result of an increase in the axial compressive force exerted on the neat MOF-5 samples because of volume expansion originating from hydrogen adsorption. Anisotropic calculations are notoriously sensitive to small changes in volumetric heat capacity when the directional properties are not too dissimilar in numerical value and when the thermal properties (i.e., conductivity and diffusivity) are on the order of insulation materials—these effects will be exacerbated when performing measurements at low temperature. Minor inaccuracies in the volumetric heat capacities with hydrogen are exacerbated with anisotropic measurements. For example, if we assume a constant hypothetical volumetric heat capacity of 0.3 MJ/m^3 K for hydrogen pressures in the range of 10–90 bar, the axial and radial thermal conductivities shown in Figure 10 are observed—*note: Figure 10 is for illustration purposes only*. Comparing Figure 8b and Figure 10 highlight the effects of a 10% reduction in the volumetric heat capacity on the overall curve shape of the axial and radial thermal conductivities. A sample volumetric heat capacity of 0.3 MJ/m^3 K at 91 bar and 16 °C correlates to a 10% reduction in the sample volumetric heat capacity in Figure 2 at the same temperature and pressure. More importantly, Figure 8b and Figure 10 demonstrate the importance of using accurate and reliable material property estimates in calculating the volumetric heat capacity.

Because we used internally consistent material property data sets from a single source for both hydrogen and helium, and used the same methodology for material property estimation; we are confident in the accuracy and precision of the estimated pressure-dependent volumetric heat capacities for helium and hydrogen. This of course assumes that both sets of hydrogen and helium data are comparable in accuracy and precision. Sensitivity of the anisotropic thermal property measurements to the volumetric heat capacity highlights the need to exercise caution when using material property data from multiple sources. We recommend using the surface fit for the specific heat capacity of hydrogen as a function of temperature and pressure (Table 3) in order to maintain consistent values within the research community. We also recommend using the equation shown Table 2 for calculating the specific heat capacity of MOF-5. The heat capacity of helium (5.19 J/g K) can be assumed constant over wide temperature (298–1000

K) and pressure (1–100 bar) ranges; however, assuming a constant helium heat capacity in the temperature range of 70–298 K and pressure range of 1–100 bar remains uncertain.

Another factor that could influence the material properties is compressive forces exerted on the sample during thermal conductivity measurements [7]. Typically, an increase in the compressive force on the sample correlates to an increase in the thermal properties in the direction of the applied force. Our neat MOF-5 samples were clamped in the axial direction as shown in Figure 1b. As previously mentioned, a consistent axial compression force was exerted on the samples using four clamping bolts tightened to a torque of 5 N•m. Attempts were made to maintain a constant applied force on the sample over the temperature and pressure range investigated with polyimide insulation (Figure 1b) to act as expansion joints. Incorporating the polyimide insulation also served as a gas diffusion layer. Hydrogen specific molecular interactions with MOF-5 may lead to a volume expansion that directly results in the increase in the axial compressive force exerted on the sample and thus affecting the observed anisotropic properties. An important point to be made is that even though we used expansion joints to accommodate volume expansions or contractions (i.e., 77K), the expansion in axial direction is constrained, wthile the expansion in the radial direction was not. Consequently, this could rationalize the observed behavior where the radial thermal properties decreased and the axial thermal properties increased with increasing hydrogen pressure beyond 20 bar. Data on the volume expansion of MOF-5 as a function of hydrogen and helium pressure would be useful for validating this hypothesis.

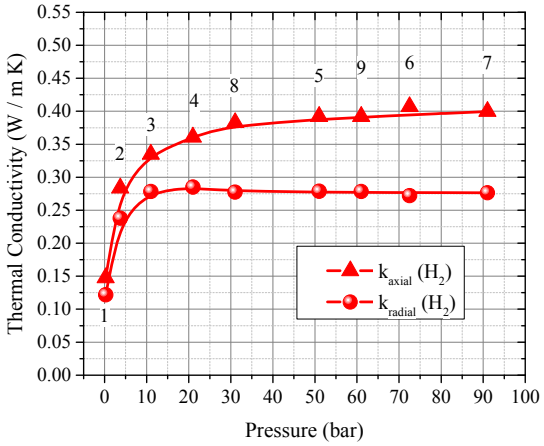

Figure 10. Recalculated anisotropic thermal conductivities of neat MOF-5 engineered compacts as a function of hydrogen pressure (absolute) at 16 °C using a constant sample volumetric heat capacity of 0.3 MJ/m^3 K in the pressure range of 10–90 bar. Note: these values are for illustration purposes only, please refer to text

4.0 Summary

The thermal conductivity measurement of MOF materials is important in the design and performance for the potential application of an on-board storage system for fuel cell vehicles. In this work, near ambient temperature (16–22 °C) thermal conductivities and diffusivities of neat MOF-5 compacts under vacuum and high pressure (≤ 90 bar) hydrogen and helium environments were presented. With the exception of the thermal properties measured under vacuum, the thermal properties should be viewed as "apparent" thermal properties— not intrinsic thermal properties. Isotropic and anisotropic thermal property measurements were performed in our in-house built high-pressure, low-temperature thermal conductivity sample cell holder using the transient plane source technique. All measurements were performed on neat MOF-5 cylindrical pucks (diameter = 5.00 cm, height = 1.312 cm) with a compacted density of 0.4 g/mL. The noteworthy points of this work can be summarized as follows:

- The measured intrinsic thermal properties of neat MOF-5 (measured under vacuum) were: Isotropic–$k_{isotropic}$ = 0.1319 W/m K, $\alpha_{isotropic}$ = 0.4165 mm^2/s; Anisotropic– k_{axial} = 0.1477 W/m K, k_{radial} = 0.1218 W/m K, α_{axial} = 0.5096 mm^2/s, and α_{radial} = 0.4232 mm^2/s

- In general, the apparent thermal properties of neat MOF-5 increased with increasing hydrogen and helium pressure, with the largest increase occurring in the narrow pressure range of 0–10 bar and then monotonically asymptoting with increasing pressures up to around 90 bar.
- On average, a greater than two-fold enhancement in the apparent thermal diffusivity and conductivity was observed with neat MOF-5 in the presence of high pressure helium and hydrogen compared to the intrinsic values of neat MOF-5 measured under vacuum—the same trend will apply to most (if not all) porous materials with low thermal properties of conductivity and diffusivity where the apparent thermal properties are dominated by the gas phase contributions
- The apparent thermal properties of neat MOF-5 measured with hydrogen were higher than those measured with helium, which were directly related to the gas-specific thermal properties of helium and hydrogen
- Neat MOF-5 exhibited a small degree of anisotropy under all conditions measured; thermal conductivities and diffusivities in the axial direction were higher than those in the radial direction
- Low temperature specific heat capacities of neat MOF-5 were measured and reported for the temperature range of -180–40 °C
- The effects of sample composition, such as additives and gas phase contributions of hydrogen and helium, must be taken into account when estimating volumetric heat capacity

In addition to our experimental findings, we also presented general methods and guidelines for measuring thermal conductivities and diffusivities under elevated pressures. Some of the important points to keep in mind when performing (and presenting) thermal conductivity research using the TPS technique include:

- Use accurate and reliable data for calculating volumetric heat capacities, clearly indicating the source of data
- Clearly state the methods and correlations used for calculating or estimating ancillary properties (e.g., density and heat capacity)
- Ensure measurements are taken under equilibrium, gradient free conditions
- Report the sample preparation, sample history, sample conditioning and sample composition
- Report the physical properties (e.g., particle size, surface area, pore volume, density, sample dimensions)
- If possible, maintain a constant compressive force on the sample over the temperature and pressure range of interest; at a minimum report the torque specification used for the initial sample loading if a bolted sample cell is used
- Be mindful of the effects of volume expansion (or contraction) related to pressure, temperature, and adsorbate-adsorbent interactions on the directional properties of thermal conductivity and diffusivity
- Use ultra-high purity gases or adsorbates to eliminate the potential confounding effects of surface contamination or sample decomposition
- Be aware that molecular interactions of the adsorbate with the adsorbent can impact the measurement of thermal conductivity (e.g., enthalpies of adsorption-desorption, adsorption site density, adsorption stoichiometry, adsorbate surface concentration…)

Acknowledgements

This work was funded by the United States Department of Energy, Office of Energy Efficiency and Renewable Energy, Fuel Cell Technologies Office. The authors gratefully acknowledge our DOE program managers Dr. Ned Stetson (Hydrogen Storage Team Lead) and Mr. Jesse Adams (DOE Golden Field Office). The authors also acknowledge the Hydrogen Storage Engineering Center of Excellence Partners for productive discussions and their dedication to hydrogen storage.

[1] T. Ragna, S. Mohn, Heat Capacity Measurements of Porous Materials at Cryogenic Temperatures, (2012).

[2] ISO/IEC, ISO 22007-2:2015 Plastics-Determination of thermal conductivity and thermal diffusivity-Part 2: Transient plane heat source (hot disc) method, 2015.

[3] D. Liu, J.J. Purewal, J. Yang, A. Sudik, S. Maurer, U. Mueller, et al., MOF-5 composites exhibiting improved thermal conductivity, Int. J. Hydrogen Energy. (2012). doi:10.1016/j.ijhydene.2011.12.129.

[4] H. Petersen, The Properties of Helium: Density, Specific Heats, Viscosity, and Thermal Conductivity at Pressures from 1 bar to 100 bar and from Room Temperature to about 1800 K, 1970.

[5] V.J. ed. Johnson, A Compendium of the Properties of Materials at Low temperature (Phase 1): Part 1-Properties of Fluids (January 1958-March 1959), 1960. http://catalog.hathitrust.org/Record/009222222.

[6] TA Intruments, Thermal Applications Note: Sapphire Specific Heat Capacity Literature Values, 1992. doi:10.1016/B978-1-4160-3779-8.10038-7.

[7] D. Garrett, H. Ban, Compressive pressure dependent anisotropic effective thermal conductivity of granular beds, Granul. Matter. 13 (2011) 685–696. doi:10.1007/s10035-011-0273-4.